VOL. 13, NO. 9, MAY 2018 ISSN 1819-6608
ARPN Journal of Engineering and Applied Sciences

www.arpnjournals.com

PRESSURE AND PRESSURE DERIVATIVE INTERPRETATION IN RADIAL NON-NEWTONIAN/NON-NEWTONIAN COMPOSITE RESERVOIRS

Freddy Humberto Escobar[1], Jesús Daniel Céspedes[1] and Alfredo Ghisays-Ruiz[2]
[1]Universidad Surcolombiana/CENIGAA, Avenida Pastrana - Cra 1, Neiva, Huila, Colombia
[2]Universidad del Atlantico, Fac. De Ciencias Básicas. Antigua vía Puerto Colombia, Barranquilla, Atlantico, Colombia
E-Mail: fescobar@usco.edu.co

ABSTRACT

Many deposits contain heavy oils that exhibit power-law non-Newtonian behavior and sometimes require the injection of another non-Newtonian fluid creating a composite system. Running pressure tests in these cases must be adequately interpreted for an accurate reservoir characterization. Application of conventional analysis would be long and tedious since it uses a Cartesian graph for each zone of the composite system and along with type-curve matching would be useless in determining the well drainage area. *TDS* technique, which can be applied separately to each region, is extended to allow the integrated interpretation of the two non-Newtonian zones and obtaining permeability, skin factor (introducing the concepts of *viscoplastic* and *viscodilatant* skin factors), distance to interface between the two zones and well drainage area. The proposed methodology was successfully verified by its application to a real case and a synthetic one.

Keywords: power law, heavy oil, pseudoplastic, dilatant, radial flow, *TDS* technique.

1. INTRODUCTION

The total crude reserves in the world are approximately formed by 40 % of heavy and extra heavy oil and other 30 % of oil sands and bitumen, (Fægestad, 2016). Despite the current low barrel prices compared to more than three years ago and the high production costs of heavy crude, the industry has focused significantly towards the production of these non-conventional deposits that are normally subject to chemical oil recovery through injection wells and are then studied by pressure transient tests, which if carried out in the most accurate way possible will bring with it a greater knowledge of the characteristics of the reservoir, better reservoir management and its economic benefit.

The literature contains numerous investigations concerning the behavior of non-Newtonian fluids in porous media. Odeh & Yang (1979) derived a partial differential equation for flow of power-law fluids through porous media. They used a power law function relating the viscosity to the shear rate. The power-law viscosity function was coupled with the variable viscosity diffusivity partial differential equation and shear rate relationship proposed by Savins (1969), generating a new partial differential equation and an approximate analytical solution. Ikoku (1979), Ikoku & Ramey (1979), Ikoku & Ramey (1979) and Ikoku & Ramey (1980), and Lund & Ikoku (1981). Okpobiri & Ikoku (1983) presented a standard work on well test analysis for non-Newtonian fluids that obey a dilatant power-law behavior, allowing well test interpretation for these reservoirs using the conventional straight-line method. However, as Gringarten (2008) pointed out, the conventional method is poor for the identification of flow regimes and has no verification; On the other hand, the standard curves method is limited to regular identifications and verifications; in contrast, *TDS* technique, using the pressure derivative, is currently the best method for both purposes.

The calculation of apparent skin factor in non-Newtonian/non-Newtonian system was recently presented by Li *et al.* (2017) using the analytical polymer injectivity model and proposed. This requires polymer rheological properties, grid size, wellbore radius, etc., and can be applied to any polymer rheology. The conducted simulation studies of polymer flooding cases to verify the concept of apparent skin factor.

Vongvuthipornchai & Raghavan (1987) used the pressure derivative method on non-Newtonian fluid pressure tests, however, the first application of the *TDS* technique, Tiab (1995) to non-Newtonian behavior was reported by Katime-Meindl & Tiab (2001). A recent application of the derivative was presented by Escobar, Martínez & Montealegre (2010), who applied the *TDS* methodology for a homogeneous radial composite deposit with a non-Newtonian / Newtonian fluid system whose first fluid follows the power law and is of character pseudoplastic. Martínez, Escobar & Cantillo (2011) presented a similar investigation, with the difference that the non-Newtonian fluid has a dilatant behavior. In addition, Escobar, Vega & Bonilla (2012) applied the same methodology for the estimation of the drainage area of a vertical well in a non-Newtonian power law crude oil field.

This paper is a continuation of the three most recently mentioned works. Then, when the industry needs to characterize a non-Newtonian crude reservoir from pressure tests when it is, for example, being tertiary recovered by injecting such non-Newtonian fluids as polymers, alkaline solutions, microemulsions or foams, this research allows giving very reliable results of permeability, skin factor, radius of injection and, if the test is long enough, drainage area. To achieve this, pressure and pressure derivative data were numerically obtained; then, characteristic features are determined to develop analytical expressions for reservoir characterization. The

new formulas are successfully verified by their application to synthetic and actual examples.

2. MATHEMATICAL MODEL

A linear partial differential equation for radial flow of non-Newtonian power-law fluids through porous media was proposed by Ikoku & Ramey (1979):

$$\frac{1}{r^n}\frac{\partial}{\partial r}\left(r^n\frac{\partial P}{\partial r}\right)=Gr^{1-n}\left(\frac{\partial P}{\partial t}\right) \quad (1)$$

This equation was applied to both reservoir zones $r_w \le r \le r_a$ and $r_a \le r \le r_e$, respectively. G and μ_{eff}, written in a general way, and adjusted to be applied with field units, are:

$$G=\frac{3792.188n\phi c_t\mu_{eff}}{k}\left(96681.605\frac{h}{qB}\right)^{\frac{1}{n}} \quad (2)$$

$$\mu_{eff}=\left(\frac{H}{12}\right)\left(9+\frac{3}{n}\right)^n\left(1.59344x10^{-12}k\phi\right)^{\frac{1-n}{2}} \quad (3)$$

Between the first zone (injection fluid) (1) and the in-situ fluid (2) there exists a transition zone or interface. Based on the criterion that they must flow at the same velocity, and since the velocity of each fluid is governed by Darcy's law for non-Newtonian fluids developed by Ikoku & Ramey (1979), this paper used the continuity condition at the interface as proposed by Lund & Ikoku (1981), obtaining:

$$\left[\lambda_{eff_1}\left(-\frac{\partial P_1}{\partial r}\right)\right]^{\frac{1}{n_1}}_{r=r_a(t)}=\left[\lambda_{eff_2}\left(-\frac{\partial P_2}{\partial r}\right)\right]^{\frac{1}{n_2}}_{r=r_a(t)} \quad (4)$$

where λ_{eff1} and λ_{eff2} are:

$$\lambda_{eff_1}=\frac{k}{\mu_{eff_1}} \quad (5)$$

$$\lambda_{eff_2}=\frac{k}{\mu_{eff_2}} \quad (6)$$

μ_{eff1} and μ_{eff2} are the effective viscosities of each fluid following the definition of Equation (3).

Since different exponents are presented on each side of the expression, the condition of the interface (Equation 4) cannot be converted into an adequate finite difference equation, so it could not be introduced into the simulator as if it were possible with the Equation (1). Then, the internal boundary condition shown by Ikoku & Ramey (1979) was rewritten in terms of apparent viscosity for each non-Newtonian fluid, μ_{app1} and μ_{app2}, as follows:

$$\mu_{app_1}=\mu_{eff_1}\left(96681.605\frac{hr}{qB}\right)^{1-n_1} \quad (7)$$

$$\mu_{app_2}=\mu_{eff_2}\left(96681.605\frac{hr}{qB}\right)^{1-n_2} \quad (8)$$

Equations (7) and (8) were substituted in Equation (4), which allowed to remove the exponents, thus obtaining a new more complete equation for the interface than that proposed by Escobar, Martínez & Bonilla (2012), with the possibility of being expressed in finite differences, compared to Equation (4):

$$\left(-\frac{\partial P_1}{\partial r}\right)_{r=r_a(t)}=\lambda\left(-\frac{\partial P_2}{\partial r}\right)_{r=r_a(t)} \quad (9)$$

where λ corresponds to:

$$\lambda=\frac{\mu_{app_1}}{\mu_{app_2}} \quad (10)$$

Finally, the expressions used by Katime & Tiab (2001) written in general terms and applied by the *TDS* methodology to find the dimensionless pressures, P_D, and dimensionless times, t_D, for the two non-Newtonian fluids are:

$$P_{DNN}=\frac{\Delta P}{141.2\left(96681.605\right)^{1-n}\left(\frac{qB}{h}\right)^n\frac{\mu_{eff}r_w^{1-n}}{k}} \quad (11)$$

$$t_{DNN}=\frac{t}{Gr_w^{3-n}} \quad (12)$$

The mathematical model considered a radial flow of two slightly compressible non-Newtonian fluids through homogeneous, isotropic and constant thickness porous media. The shape of the reservoir is cylindrical with finite external radius and non-flow boundary. A fluid flows at a constant rate through a well in the center of the reservoir and the other fluid corresponds to the in-situ fluid. Figure-1 is a schematic representation of the reservoir under consideration.

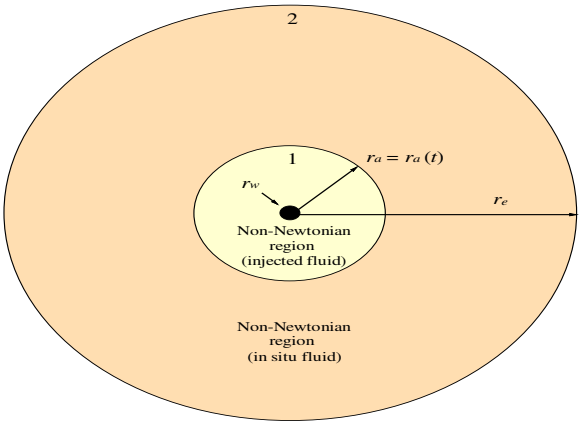

Figure-1. Non-Newtonian/non-Newtonian radial composite reservoir diagram.

3. PRESSURE DERIVATIVE BEHAVIOR

The pressure derivative curves of a non-Newtonian fluid differ from the shape of the curves of a Newtonian fluid. While a Newtonian fluid (flow behavior index, $n = 1$) has a slope equal to zero, a fluid that follows the power law of pseudoplastic behavior ($0 < n < 1$) has a positive slope straight line which increases as its flow behavior index declines, as shown by Katime-Meindl & Tiab (2001). On the other hand, a dilatant fluid ($1 < n < 2$) has an increasingly negative slope as its index increases, according to Martínez *et al*. (2011). This behavior is also kept for the two fluids under study as shown in Figure-2.

A transition zone occurred between the radial flows of the two non-Newtonian fluids. This was influenced by the consistency indexes H_1 and H_2 of each fluid. With $H_1 < H_2$, the slope tended to have a positive value, however with $H_1 > H_2$, the slope of the transition tended to be negative. With the condition $H_1 = H_2$, in most cases a defined slope of transition between the two flows was not observed. (See Figure-3).

From further observations on both pseudoplastic and dilatant fluids, the smaller n_1 value, the shorter the time required to reach the beginning of the transition, however, not necessarily faster is reached radial flow of the in-situ fluid. Also, as H_2 decreases, the pseudosteady-state period is reached more rapidly.

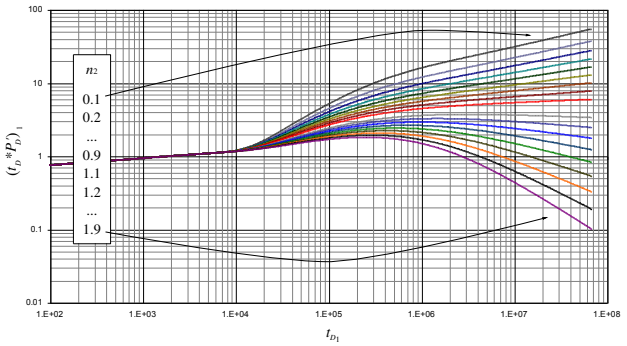

Figure-2. Dimensionless pressure derivative behavior of pseudoplastic non-Newtonian fluids, $n_1 = 0.8$, $H_1 = 30$ cP*s^{n-1} and $H_2 = 100$ cP*s^{n-1}

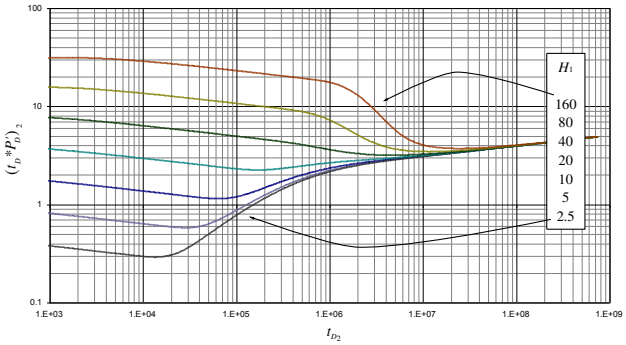

Figure-3. Dimensionless pressure derivative behavior of a dilatant non-Newtonian and pseudoplastic non-Newtonian fluids, $n_1 = 1.2$, $n_2 = 0.75$ and $H_2 = 20$ cP*s^{n-1}

The dimensionless time and pressure derivative values can be found with the flow indexes of the first or second fluid. When the well fluid is studied by varying some of its flow behavior indexes, a better and simpler interpretation of the behavior of the dimensionless curves is achieved by t_D and t_D*P_D ' with the data of the second fluid n_2 and H_2, as shown in Figure 3. Otherwise, when the in-situ fluid to which any of its two indexes are varied, both t_D and t_D*P_D' must be found with n_1 y H_1, as shown in Figure-2.

4. APPLICATION OF *TDS* TECHNIQUE

According to Katime-Meindl & Tiab (2001), the dimensionless equation for a radial flow regime of a power-law non-Newtonian fluid is:

$$\left(t_D * P_D{}'\right)_{rNN} = 0.00708\left(96681.605\right)^{n-1}\left(\frac{h}{qB}\right)^{n} \frac{k}{\mu_{eff}} r_w^{n-1}\left(t*\Delta P'\right)_{rNN} \quad (13)$$

The value of this same dimensionless pressure derivative of after being presented in a log-log plot of t_D*P_D' against (t_D) is:

$$\left(t_D * P_D{}'\right)_{rNN} = 0.5 t_{DNN}^{\alpha} \quad (14)$$

α is the slope of the pressure derivative curve on the non-Newtonian region and defined as:

$$\alpha = \frac{1-n}{3-n} \quad (15)$$

Equation (14) was proposed for both non-Newtonian fluids. Both equations were equated to 0.5, obtaining:

$$\frac{\left(t_D * P_D{}'\right)_{r_1}}{t_{D_1}^{\alpha_1}} = \frac{\left(t_D * P_D{}'\right)_{r_2}}{t_{D_2}^{\alpha_2}} \tag{16}$$

Where $(t_D*P_D')_1$ and $(t_D*P_D')_2$ follow the definition of Equation (14), t_{D1} and t_{D2} follow the definition of Equation (12), and α_1 and α_2 follow the definition of Equation (16). $(t*\Delta P')_1 = (t*\Delta P')_2$ and $t_1 = t_2$, and finally, the permeability was finally obtained:

$$k = \left\{ \begin{array}{l} \left(96681.605\dfrac{h}{qB}\right)^{n_1-n_2} \\ \left(t_{irNN\_NN}\right)^{\alpha_2-\alpha_1} \\ \left(\dfrac{\mu_{eff_1}^{*\,\alpha_1-1}}{\mu_{eff_2}^{*\,\alpha_2-1}}\right)\left(\dfrac{G_1^{*\alpha_1}}{G_2^{*\alpha_2}}\right) \end{array} \right\}^{\frac{1}{(\alpha_1-\alpha_2)+\frac{1}{2}\left[(n_2-n_1)+\alpha_2(1-n_2)-\alpha_1(1-n_1)\right]}} \tag{17}$$

Where t_{irNN_NN} is the time of the point of intersection between the slopes of the two non-Newtonian fluids in a log-log plot of $t*\Delta P'$ vs. t, and where μ^*_{eff1}, μ^*_{eff2}, G^*_1, and G^*_2, are:

$$\mu_{eff_1}^{*} = \left(\frac{H_1}{12}\right)\left(9+\frac{3}{n_1}\right)^{n_1}\left(1.59344\times10^{-12}\phi\right)^{\frac{1-n_1}{2}} \tag{18}$$

$$\mu_{eff_2}^{*} = \left(\frac{H_2}{12}\right)\left(9+\frac{3}{n_2}\right)^{n_2}\left(1.59344\times10^{-12}\phi\right)^{\frac{1-n_2}{2}} \tag{19}$$

$$G_1^{*} = 3792.188 n_1 \phi c_t \left(96681.605\frac{h}{qB}\right)^{\frac{1}{n_1}} \tag{20}$$

$$G_2^{*} = 3792.188 n_2 \phi c_t \left(96681.605\frac{h}{qB}\right)^{\frac{1}{n_2}} \tag{21}$$

Equation (17) is not applicable for $n_1 = n_2$, because at the occurrence of such a condition the slopes of the two flows are parallel and, therefore, never converge to a common point. The permeability value and skin factor obtained from the radial flow of a non-Newtonian fluid can be estimated from the Equations presented by Escobar *et al*. (2010) and Escobar, Martínez & Bonilla (2012):

$$k = \left(\left[\begin{array}{l} 70.6\left(96681.605\right)^{(1-\alpha)(1-n)} \\ \left(\dfrac{0.0002637 t_{rNN}}{n\phi c_t}\right)^{\alpha} \\ \left(\dfrac{qB}{h}\right)^{n-\alpha(n-1)}\left(\dfrac{r_w^{\alpha(n-3)+(1-n)}}{\left(t*\Delta P'\right)_{rNN}}\right) \end{array} \right]^{\frac{1}{1-\alpha}} \left(\left(\frac{H}{12}\right)\left(9+\frac{3}{n}\right)^{n}\left(1.59344\times10^{-12}\phi\right)^{\frac{1-n}{2}}\right) \right)^{\frac{2}{1+n}} \tag{22}$$

$$s = \frac{1}{2}\left(\left(\frac{\Delta P}{\left(t*\Delta P'\right)}\right)_{rNN} - \frac{1}{\alpha}\right)\left(\frac{t_{rNN}}{G r_w^{3-n}}\right)^{\alpha} \tag{23}$$

Equations (22) and (23) apply to both non-Newtonian fluids taking care of using the properties of each zone.

Escobar *et al*. (2010) and Martínez *et al.* (2011) proposed expressions that allow finding the distance from the well to the interface of the pseudoplastic and dilatant injection fluid, respectively, in a non-Newtonian / Newtonian system. The expressions adjusted for the present case are:

$$r_a = \left[\frac{G_1\left(\begin{array}{l} 0.2258731 n_1^3 - 0.2734284 n_1^2 + \\ 0.5064602 n_1 + 0.5178275 \end{array}\right)^{\frac{1}{\alpha_1}}}{t_*} \right]^{\frac{1}{n_1-3}} \tag{24}$$

$$r_a = \left[\frac{G_1\left(0.46811 e^{0.76241 n_1}\right)^{\frac{1}{\alpha_1}}}{t_{e\_rNN1}} \right]^{\frac{1}{n_1-3}} \tag{25}$$

Equation (24) applies for pseudoplastic fluid and Equation (25) for dilatant fluids. t_* in Equation (24) ought to be replaced for one of the following times:

- Time of the maximum curvature point at the beginning of the transition t_{MC}
- Time of the maximum derivative point of the transition t_M
- Time of the point of intersection between the slopes of the injection fluid and the transition between the two radial flows t_{irNN1_Tr}

The expression provided by Escobar *et al.* (2012) for the drainage area determination also applies here:

$$A = \pi \left[\frac{t_{rpiNN_2}}{G_2} \left(\frac{1}{4} \right)^{\frac{1}{\alpha_2 - 1}} \right]^{\frac{2}{3-n_2}} \quad (26)$$

5. APPROPRIATE USE OF THE EXPRESSIONS

An accuracy analysis was performed on all the expressions due to the great variety of situations that can occur in a reservoir with two non-Newtonian fluids. This variety of cases depends mainly on fluid type. If the fluids in zones 1 and 2 are either pseudoplastic or dilatant types or a combination of both; condition that is given by the flow behavior indexes n_1 and n_2. The value of the two consistency indexes H_1 and H_2. That is, if the index of the fluid in zone 1 has a value greater, less than or equal to that of the second zone. This classification is given in Table-1.

Permeability estimated with Equations (17) and (22) apply with great accuracy for all cases given in Table-1. Same situation occurs with skin factor and drainage area estimations.

It was observed that the two skin factors of zones 1 and 2 presented a certain tendency of dependence against their respective values of flow index behavior and of independence against their respective values of index of consistency and the remaining fluid and petrophysical values. That is to say, as n changed, the skin factor was seen affected, and when H or another parameter was doing it, the skin factor tended to remain constant. However, the modification of n or H of the zone 1 fluid caused an additional variation in the skin factor of the second zone, so that when n_1 or H_1 increased, the second zone skin factor did likewise.

Based on the described criterion, the skin factor of zone 1, for all twelve cases, can be calculated correctly since if the value of the flow behavior index n_1 is kept fixed regardless of the value of the consistency index H_1 or another parameter, the skin factor is the same. Otherwise, by varying n_1 and keeping H_1 fixed, the skin factor undergoes gradual and coherent changes. In fact, that exclusive dependence of zone 1 as a function of the flow behavior index is reflected in a single value of s_1 for each n_1. Table-2 and Figure-4 show these values. The skin factor values shown in Table-2 would also be displayed in reservoirs with a single non-Newtonian fluid. As can be seen, negative values of s_1 were produced by pseudoplastic fluids while positive values were present in dilating fluids. For both pseudoplastic and dilatant fluids, as n_1 increased, the respective skin factor decreased.

On the other hand, with regard to the skin factor of the zone 2, apart from the additional variation that occurred in all cases, the mentioned criterion was only glimpsed and for which correct results are inferred (besides being consistent) in cases 5, 6, 9 and 12. Also, the criterion was fulfilled in cases 2 and 3 only if n_1 was less than n_2. As can be seen, it is possible to conclude that the criterion tends to be visualized in cases where $H_1 < H_2$ and $H_1 = H_2$ and also especially when $n_1 < n_2$. For both pseudoplastic and dilatant fluids, as n_2 increased, the respective skin factor decreased.

The index n, being a property of the fluid that intervenes deeply in the flow and liquid velocity liquid, has allowed by means of said aforementioned dependence to speak of what could be classified as *viscoplastic skin factor* generated by pseudoplastic fluids, and *viscodilatant skin factor* generated by dilatant fluids, at distances distant from the well in both zones.

As far as the distance to the interface is concerned, cases 1 to 6 were worked with *Equation* 24 because the first fluid is pseudoplastic, while for cases 7 to 12, Equation (25) was used since in these the first fluid corresponds to a dilatant. As mentioned above, the calculation of the radius with Equation (25) can be performed with t_{MC}, t_M or t_{irNN1_Tr}, depending on the case.

Table-1. Possible cases given in a reservoir with two non-Newtonian zones.

Case	Non-Newtonian fluid		Consistency index, H		
	Zone 1	Zone 2	Zone 1		Zone 2
1	Pseudoplastic	Pseudoplastic	H_1	>	H_2
2	Pseudoplastic	Pseudoplastic	H_1	<	H_2
3	Pseudoplastic	Pseudoplastic	H_1	=	H_2
4	Pseudoplastic	Dilatant	H_1	>	H_2
5	Pseudoplastic	Dilatant	H_1	<	H_2
6	Pseudoplastic	Dilatant	H_1	=	H_2
7	Dilatant	Pseudoplastic	H_1	>	H_2
8	Dilatant	Pseudoplastic	H_1	<	H_2
9	Dilatant	Pseudoplastic	H_1	=	H_2
10	Dilatant	Dilatant	H_1	>	H_2
11	Dilatant	Dilatant	H_1	<	H_2
12	Dilatant	Dilatant	H_1	=	H_2

Table-2. Skin factor presented in Zone 1.

Pseudoplastic		Dilatant	
n_1	s_1	n_1	s_1
0.1	-1.08	1.1	9.9
0.2	-1.22	1.2	4.87
0.3	-1.41	1.3	3.19
0.4	-1.65	1.4	2.33
0.5	-1.99	1.5	1.81
0.6	-2.5	1.6	1.45
0.7	-3.34	1.7	1.2
0.8	-5.02	1.8	1.02
0.9	-10.02	1.9	0.91

Table-3. Fluid and reservoir properties for both examples.

Parameter	Synthetic example	Field example	Parameter	Synthetic example	Field example
P_r, psi	2 000	2 500	t, días	120	8.98
r_e, ft	3 000	2 625	q, Bbl/día	125	300
r_a, ft	100	131.2	B, rb/STB	1.2	1
r_w, ft	0.4	0.33	n_1	0.8	0.6
h, ft	20	16.4	H_1, cP*s^{n-1}	40	20
ϕ, %	0.25	20	n_2	1.5	1
k, md	500	100	H_2, cP*s^{n-1}	200	3
c_t, 1/psi	5.5x10^{-6}	6.89x10^{-6}			

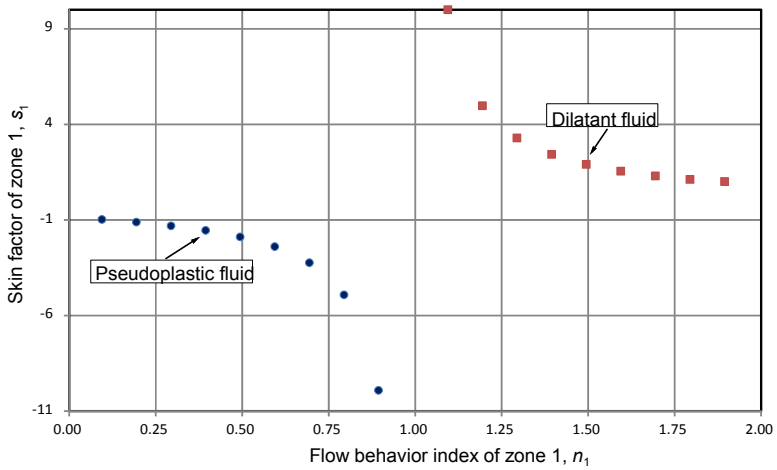

Figure-4. Flow behavior index of zone 1, n_1 vs. skin factor of zone 1, s_1.

Case 1: A point of maximum curvature is generated immediately after the radial flow slope of the injection fluid. The time corresponding to that point of maximum curvature t_{MC} allowed finding the distance from the well to the interface. In most situations, the t_{MC} corresponds to the time of the maximum derivative point in the transition t_M.

Cases 2 and 5: The time of the point of intersection between the first flow and the transition between the two radial flows t_{irNN1_Tr}, made possible the r_a calculation. However, for both cases, as the two flow behavior indexes moved away from each other and the two consistency indexes approached significantly, and the condition $n_1 < n_2$ for case 2 was presented, the transition presented at the beginning an additional slope. The intersection must be constructed by extrapolating that slope.

Cases 3 and 6: To calculate r_a, the time of the intersection point between the first flow and the transition between the two radial flows t_{irNN1_Tr} must be used. As in cases 2 and 5, as the two flow indexes moved away from each other and the condition $n_1 < n_2$ for case 3 was present, the transition initially had an additional slope. The intersection must be constructed by extrapolating that slope.

Case 4: The pressure derivative curve has a maximum located after the first radial flow, as is usually the case in case 1. The time corresponding to that maximum pressure derivative value t_M allows estimating r_a.

Cases 7 to 12: Equation (25) generated reliable values of radius for all cases when fluid 1 has dilatant behavior.

6. EXAMPLES

A constant flow injection test in a heavy oil field with closed boundaries was generated and interpreted. The input simulation data are shown in Table-3. In addition, a constant flow injection test performed by Lund & Ikoku (1981) with the information given in Table-3 was also worked on. The objective is to characterize both tests.

Synthetic example. The example presents a system which injection fluid exhibits a pseudoplastic behavior while the in-situ fluid behaves as a dilatant fluid. Figure-5 corresponds to the log-log plot of the pressure and pressure derivative versus injection time curves. Case 5 of Table-1 is dealt. Therefore, the injection radius must be found by Equation (25). The following data points were read from Figure-5.

t_1 = 0.10011 hr $(t^*\Delta P')_1$ = 34.2572 psi $(\Delta P)_1$ = 217.2565 psi
t_2 = 500.2699 psi $(t^*\Delta P')_2$ = 56.9775 psi $(\Delta P)_2$ =748.8741 psi
t_{irNN_NN} = 220 hr $\boldsymbol{t_{irNN1\_Tr}}$ = 0.82 hr t_{rpiNN2} =1 400 hr

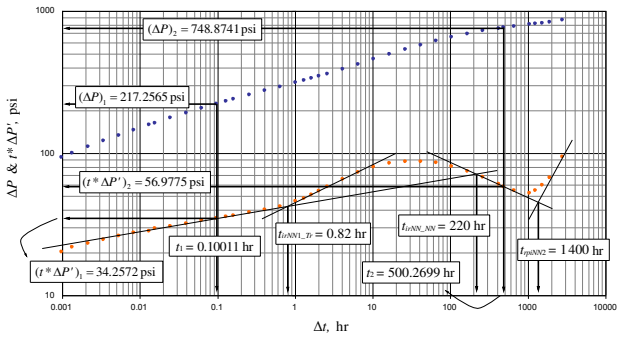

Figure-5. Log-log plot of pressure and pressure derivative versus time for the synthetic example.

First, α values of 0.09 for the injection fluid and -0.33 for the in-situ fluid are calculated with Equation (16), based on their respective flow behavior indexes n_1 and n_2. Then, using Equations (18), (19), (20) and (21) μ^*_{eff1}, μ^*_{eff2}, G^*_1, and G^*_2 are found to be 1.47, 765 365.981, 0.0277 and 6.88878x10^{-5}, respectively. Using the above calculated parameters and the time of intersection between the two radial flows t_{irNN_NN}, the permeability is estimated by Equation (17).

$$k = \left\{ \left(96681.605 \frac{20}{(125)(1.2)} \right)^{0.8-1.5} (220)^{-0.\overline{33}-0.\overline{09}} \left(\frac{(1.47)^{0.\overline{09}-1}}{(765365.981)^{-0.\overline{33}-1}} \right) \left(\frac{(0.0277)^{0.\overline{09}}}{(6.88878\times10^{-5})^{-0.\overline{33}}} \right) \right\}^{\frac{1}{(0.\overline{09}-(-0.\overline{33}))+\frac{1}{2}\left[(1.5-0.8)+(-0.\overline{33})(1.5-1)-0.\overline{09}(1-0.8)\right]}}$$

$$= 504.33 \text{ mD}$$

Permeability is verified by applying Equation (22) to both radial flow regimes:

$$k = \left(\left[70.6\left(96681.605\right)^{(1-0.\overline{09})(1-0.8)} \left(\frac{0.0002637(0.1011)}{(0.8)(0.25)(5.5\times10^{-6})} \right)^{0.\overline{09}} \left(\frac{(125)(1.2)}{(20)} \right)^{0.8-0.\overline{09}(0.8-1)} \left(\frac{0.4^{0.\overline{09}(0.8-3)+(1-0.8)}}{34.2572} \right) \right]^{\frac{1}{1-0.\overline{09}}} \left(\left(\frac{40}{12} \right) \left(9+\frac{3}{0.8} \right)^{0.8} \left(1.59344\times10^{-12}(0.25) \right)^{\frac{1-0.8}{2}} \right) \right)^{\frac{2}{1+0.8}} = 508.18 \text{ md}$$

$$k = \left(\left[70.6\left(96681.605\right)^{(1-(-0.\overline{33}))(1-1.5)} \left(\frac{0.0002637(500.2699)}{(1.5)(0.25)(5.5\times10^{-6})} \right)^{-0.\overline{33}} \left(\frac{(125)(1.2)}{(20)} \right)^{1.5-(-0.\overline{33})(1.5-1)} \left(\frac{0.4^{(-0.\overline{33})(1.5-3)+(1-1.5)}}{56.9775} \right) \right]^{\frac{1}{1-(-0.\overline{33})}} \left(\left(\frac{200}{12} \right) \left(9+\frac{3}{1.5} \right)^{1.5} \left(1.59344\times10^{-12}(0.25) \right)^{\frac{1-1.5}{2}} \right) \right)^{\frac{2}{1+1.5}} = 481.61 \text{ md}$$

The resulting averaged permeability is k = 498.04 md which will be used in the following calculations. Then, the effective viscosities are found with Equation (3) and G parameters with Equation (2) to be 2.736 cp*(s/ft)$^{n-1}$, 162 014.207 cp*(s/ft)$^{n-1}$, 0.0001521 hr/ft^{3-n} and 0.02241 hr/ft^{3-n}, respectively.

Application of Equation (23) to both radial flow regimes allows finding the skin factor:

$$s_1 = \frac{1}{2}\left(\left(\frac{217.2565}{34.2572} \right) - \frac{1}{0.\overline{09}} \right) \left(\frac{0.10011}{(0.0001521)(0.4)^{3-0.8}} \right)^{0.\overline{09}} = -5.05$$

$$s_2 = \frac{1}{2}\left(\left(\frac{748.8741}{56.9775} \right) - \frac{1}{-0.\overline{33}} \right) \left(\frac{500.2699}{(0.02241)(0.4)^{3-1.5}} \right)^{-0.\overline{33}} = 0.18$$

As confirmed here, the skin factor s_1 = -5.05 agrees with what is stated in Table-2.

The distance from the well to the interface is found with Equation (24) and the drainage area with Equation (26):

$$r_a = \left[\frac{0.0001521\left(\frac{0.2258731(0.8)^3 - 0.2734284(0.8)^2 + 0.5064602(0.8) + 0.5178275}{0.82} \right)^{\frac{1}{0.\overline{09}}}}{} \right]^{\frac{1}{0.8-3}}$$

$$= 103.4 \text{ ft}$$

$$A = \pi \left[\frac{1400}{0.02241} \left(\frac{1}{4} \right)^{\frac{1}{(-0.\overline{33})-1}} \right]^{\frac{2}{3-1.5}} = 715.13 \text{ acres}$$

Field case example. Lund & Ikoku (1981) presents an example consisting of a non-Newtonian injection fluid of pseudoplastic character and an in-situ fluid of Newtonian behavior, nevertheless the expressions formulated here with the exception of Equation (23) (skin factor in the in-situ zone), accept a n_2 = 1. Figure-6 contains the log-log plot of pressure and pressure derivative vs. time for this example from which the following data were read:

t_1 = 0.10011 hr $(t*\Delta P')_1$ = 86.9221 psi $(\Delta P)_1$ = 439.292 psi
t_2 = 50.05438 hr $(t*\Delta P')_2$ = 39.1849 psi $(\Delta P)_2$ = 966.327 psi
t_{irNN_NN} = 0.00077 hr t_M, t_{MC} = 1.28138 hr

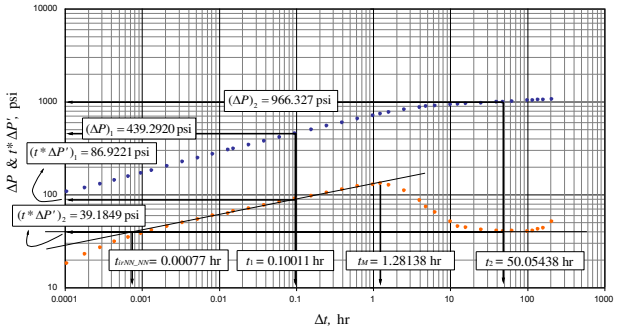

Figure-6. Log-log plot of pressure and pressure derivative versus time for the actual field example.

Permeability is found with Equations (17) and (22) –last one twice- to be, k = 97.21, 101.92 and 98.87 which averaged value is k = 99.3333 md. The skin factor

in the injection zone resulted to be, s_1 = -2.52, using Equation (23). As for the former example, the skin factor values agrees with that stated in Table-2. Equation 2.34 by Tiab (1995) allows finding the skin factor in the Newtonian zone. According to Escobar et al (2010), this expression applied to the nomenclature of this paper is:

$$s_2 = \frac{1}{2}\left[\left(\frac{\Delta P}{t*\Delta P'}\right)_{r_2} - \ln\left(\frac{k_2 t_{r_2}}{\phi\mu_N c_t r_w^2}\right) + 7.43\right] \quad (27)$$

$$s_2 = \frac{1}{2}\left[\left(\frac{966.327}{39.1849}\right) - \ln\left(\frac{(99.\overline{33})(50.05438)}{(0.2)(3)(6.89\times10^{-6})(0.33)^2}\right) + 7.43\right] = 4.48$$

As a specific value of n_1 in the non-Newtonian zone generates a specific skin factors which are shown in Table-2, further analysis by Equation (27) allowed observing that a Newtonian zone always presents a zero skin factor. That is, for n_1 = 1, s_1 = 0. For this pseudoplastic/Newtonian system, the injection radius is found with Equation (24) using the time value at the maximum pressure derivative point, t_M, which results to be r_a = 119.28 ft. No drainage area is estimated since pseudosteady state is unreached. As seen in both examples the mechanical skin factor ought to be the same; then, this implies the existence of a pseudoskin factor created by the nature of the fluid. These can be called *viscoplastic* and *viscodilatant* skin factors.

7. CONCLUSIONES

a) *TDS* Technique was implemented for the interpretation of pressure tests in non-Newtonian/non-Newtonian composite systems. The analysis of the pressure derivative curve allowed identifying specific characteristics in this, more precisely the point of intersection between the slopes of the two radial non-Newtonian flows, which led to find a new analytical expression for the calculation of formation permeability. The *TDS* Technique for these systems involves the application to 12 different scenarios depending on the fluid characteristics.

b) The concepts of viscoplastic and viscodilatant skin factors, generated by the non-Newtonian character of the power-law fluids under consideration, were introduced. Besides, a pseudoplastic character produces stimulation and a dilatant behavior causes additional skin factor (well damage).

ACKNOWLEDGEMENTS

The authors express their most sincere thanks to God, Universidad Surcolombiana and Universidad del Atlántico for the completion of this work.

REFERENCES

Escobar F.H., Martínez J.A. and Bonilla L.F. 2012. Numerical Solution for a Radial Composite Reservoir Model with a No-Newtonian/Newtonian Interface. Journal of Engineering and Applied Sciences. 7(8).

Escobar F.H., Martínez J.A. and Montealegre-M. M. 2010. Pressure and Pressure Derivative Analysis for a Well in a Radial Composite Reservoir with a Non-Newtonian/Newtonian Interface. CT&F. 4(1): 33-42.

Escobar F.H. 2012. Transient Pressure and Pressure Derivative Analysis for Non-Newtonian Fluids, in: Gomes, J.S. (Ed.), New Technologies in the Oil and Gas Industry. In. Tech, Rijeka, p. Ch. 07. DOI: 10.5772/50415.

Escobar F.H., Bonilla D.F. and Cicery Y.Y. 2012. Pressure and Pressure Derivative Analysis for Pseudoplastic Fluids in Vertical Fractured Wells. Journal of Engineering and Applied Sciences. 7(8).

Escobar F.H., Martinez A., and Silva D.M. 2013. Conventional Pressure Analysis for Naturally-Fractured Reservoirs with Non-Newtonian Pseudoplastic Fluids. 11(1). Fuentes Journal. pp. 27-34.

Escobar F.H., Martinez J.A. and Bonilla L.F. 2012. Transient Pressure Analysis for Vertical Wells with Spherical Power-Law Flow. CT&F. 5(1): 19-25.

Escobar F.H., Vega L.J. and Bonilla L.F. 2012. Determination of Well-Drainage Area for Power-Law Fluids by Transient Pressure Analysis. CT&F. 5(1): 45-55.

Gringarten A. C. 2008. From Straight Lines to Deconvolution: The Evolution of the State of the Art in Well Test Analysis. SPE Reservoir Evaluation and Engineering, 11(1), 41-62. Society of Petroleum Engineers. DOI: 10.2118/102079-PA.

Ikoku C. U. 1979, January 1. Practical Application of Non-Newtonian Transient Flow Analysis. Society of Petroleum Engineers. DOI: 10.2118/8351-MS.

Ikoku C. U. and Ramey H. J. 1979, June 1. Transient Flow of Non-Newtonian Power-Law Fluids in Porous Media. . Society of Petroleum Engineers Journal, 19(3): 164-174. Society of Petroleum Engineers. DOI: 10.2118/7139-PA.

Ikoku C. U., and Ramey H. J. 1980, February 1. Wellbore Storage and Skin Effects during the Transient Flow of Non-Newtonian Power-Law Fluids in Porous Media. Society of Petroleum Engineers Journal 20(1): 25-38. Society of Petroleum Engineers. DOI: 10.2118/7449-PA.

Katime-Meindl I. and Tiab D. 2001, January 1. Analysis of Pressure Transient Test of Non-Newtonian Fluids in Infinite Reservoir and in the Presence of a Single Linear

Boundary by the Direct Synthesis Technique. Society of Petroleum Engineers. DOI: 10.2118/71587-MS.

Li Z., Fortenberry R., Luo H., Delshad M. 2017. An examination of the concept of apparent skin factor in modeling injectivity of non-Newtonian polymer solutions. Journal of Petroleum Science and Engineering. doi: 10.1016/j.petrol.2017.08.044.

Lund O. and Ikoku C. U. 1981, April 1. Pressure Transient Behavior of Non-Newtonian/Newtonian Fluid Composite Reservoirs. Society of Petroleum Engineers Journal, 21(2): 271-280. Society of Petroleum Engineers. DOI: 10.2118/9401-PA.

Martinez J.A., Escobar F.H. and Cantillo J.H. 2011. Application of the TDS Technique to Dilatant Non-Newtonian/Newtonian Fluid Composite Reservoirs. Ingeniería e Investigation journal. 31(3): 130-134.

Odeh A. S. and Yang H. T. 1979, June 1. Flow of Non-Newtonian Power-Law Fluids through Porous Media. Society of Petroleum Engineers Journal, 19(3): 155-163. Society of Petroleum Engineers. DOI: 10.2118/7150-PA.

Okpobiri G. A. and Ikoku C. U. 1983, January 1. Pressure Transient Behavior of Dilatant Non-Newtonian/ Newtonian Fluid Composite Reservoirs. Society of Petroleum Engineers. DOI: 10.2118/12307-MS.

Savins J. G. 1969. Non-Newtonian Flow through Porous Media. Industrial and Engineering Chemistry. 61(10): 18-47. DOI: 10.1021/ie50718a005.

Tiab D. 1995. Analysis of Pressure and Pressure Derivative without Type-Curve Matching: 1- Skin and Wellbore Storage. Journal of Petroleum Science and Engineering. 12: 171-181.

Vongvuthipornchai S. and Raghavan R. 1987, December 1. Well Test Analysis of Data Dominated by Storage and Skin: Non-Newtonian Power-Law uids. SPE Formation Evaluation. 2(4): 618-628. Society of Petroleum Engineers. DOI: 10.2118/14454-PA.

Nomenclature

B	Liquid formation factor, rb/STB
c_t	Total compressibility, 1/psi
h	Formation thickness, ft
H	Consistency index, $cP*s^{n-1}$
k	Permeability, md
n	Power-law index or flow behavior index
P	Pressure, psi
q	Flow rate, BPD
r	Radius, ft
r_a	Radius from well to the interface formed between the two fluids
s	Skin factor
t	Time, hr
$t*\Delta P'$	Pressure derivative, psi
t_D*P_D'	Dimensionless pressure derivative

Greek

α	Pressure derivative slope during non-Newtonian radial flow
Δ	Change, drop
λ	Apparent mobility ratio
λ_{eff}	Effective movility, $[cP*(s/ft)^{n-1}]$/md
μ	Viscosity, cp
μ_{app}	Apparent viscosity, cp
μ_{eff}	Effective viscosity, $cp*(s/ft)^{n-1}$
ϕ	Porosity, fracción

Subscripts

1	Zone 1 or near-wellbore fluid
2	Zone 2 or in-situ fluid
a	Interface location
app	Apparent
C	Curvature
D	Dimensionless
e	External
e_r	End of radial flow
eff	Effective
*e_rNN*1	Ending time of zone 1
i	Intersection
irNN_NN	Intersection between the slopes of the two non-Newtonian fluids
M	Maximum
NN	No-Newtonian
p	Pseudosteady state
r	Radial flow
*rpiNN*2	Intersection between the second zone radial flow and the pseudosteady-state period
Tr	Transition
w	Well